Effect of dye sensitization's temperature on ZnO-based solar cells

Anurag Roy,* Senthilarasu Sundaram, Tapas K. Mallick

Environment and Sustainable Institute, University of Exeter, Penryn Campus, Cornwall TR10 9FE, U.K.

Email: A.Roy30@exeter.ac.uk

ABSTRACT

We have investigated the insights of photo-physical surface characteristics for Ru (II) polypyridyl dye (N719) sensitization and its performance in dye-sensitized solar cells (DSSCs) at different temperatures of ZnO-based photoanodes. The maximum power conversion efficiency of 2.25% with a high open-circuit voltage of 0.87 V was recorded for 40^{o}C sensitized device under 1SUN 1.5 AM. The 60^{o}C sensitized device shows the maximum current density of 8.8 mA.cm^{-2} and 25^{o}C sensitized device results. Therefore, the mode of surface interaction of N719-ZnO to promote better electron conduction has highlighted the prospects of DSSCs under diverse solution sensitization temperature environment.

Keywords: DSSC; N719 dye; Sensitized; Surface interaction; ZnO,

Introduction

Temperature is probably the essential outdoor variable that affects the photovoltaic performance of the DSSCs. There are some vital external effects like temperature, moisture, the intensity of sunlight exposure, and photo-corrosion, directly influencing the solar cell limiting parameters and charge transport mechanism in DSSCs [1,2]. The effect of temperature on sensitization of metal-organic dye molecule on a nanocrystalline ZnO based photoanode is focused in this section. In general, DSSCs are evaluated under one sun illumination. Still, the temperature of the DSSC during its characterization is often not specified, even though temperature strongly influences physical parameters, like the hole diffusion in the electrolyte and/or recombination reactions of the generated electrons in the electrolyte, dye stability, photobleaching etc. The most widely used photosensitizers are Ru (II) polypyridyl dye., i.e., Di-tetrabutylammonium cis-bis(isothiocyanato)bis(2,2′-bipyridyl-4,4′-dicarboxylato) ruthenium (II) or N719 where the light absorption originates due to MLCT process with molar extinction coefficient (ε) of 10,000-20,000 M-1cm-1 [3]. Functionalizing the ancillary polypyridyl ligand by the substituents including alkyl, aryl, alkoxy, phenyl, heterocycle etc., or by replacing the chelating anions many popular dyes such as N719, N3, N749 (black dye), Z907, K51, K60, N886, C103, JK56 etc. have been synthesized. A maximum of 12.4% power conversion efficiency (PCE) has been reported to be achieved with these Ru (II) dye-based DSSCs till 2010 [4-8]. Multiple anchoring moieties such as hydroxyl, carboxylate, phenolic-OH, thiocyanates etc., of different sensitizers are responsible for such strong electrostatic interaction. Various studies reported the vulnerable nature of ZnO in acidic environments resulting in the formation of Zn^{2+}/dye aggregates during sensitization [9-13].

Numerous efforts are going on for changing metal and designing the ligand to increase the stability, molar extinction coefficient and reduce the cost of the metal complex photosensitizes. N719 dye molecule with high electrostatic interaction with the photoanode surface is the

critical component that gets degraded with time and temperature. In general, the dye loading on a photoanode depends on the nature and number of anchoring groups of the dyes in addition to the surface characteristics of the photoanode [14, 15]. To increase and optimize the photochemical performance of a DSSC device, it is necessary to make sure effective and maximum dye loading on the photoanode without the formation of dye aggregates during adsorption. It is not always easy to fabricate a device and evaluate its performance for zingoptimizing the dye loading conditions.

Attempts have been made to understand the effect of temperature on the dye molecules' interaction with the photoanode. It is quite apparent that enhanced temperature accelerates the sensitization process, but at the same time, there is an extensive possibility for dissociation of the dyes. Various characterization and techniques are evolved to understand further the actual interaction mechanism of dye molecules and oxides. Lee et al. (2010) reported N719 dye adsorption understanding behaviour towards anatase TiO_2 through Fourier-transform infrared spectroscopy (FTIR) and confocal Raman spectroscopic studies [16]. In contrast, Hirose et al. (2010) performed temperature-dependent systematic FTIR studies for N719 dye sensitization [17]. Yoshida et al. (2012) revealed light exposure and heat treatment during the N179 dye sensitization process [18]. Another work by Berginc et al. (2008) demonstrated the electrolyte concentrations assisted by temperature as a mean to improve the device performance [19] significantly. Here, the effect of temperature on dye sensitization and its impact on DSSC performance has been investigated in details.

Various physicochemical investigations were performed to describe the surface interaction behavior of ZnO-N719 dye for different sensitization temperature. We have observed the significant influence of sensitization temperature over the solar cell’s overall parameters and finally the PCE. In this report, we try to sort the photoanode - dye interaction in the ZnO-N719

dye-based system and other dye loading behaviour towards their overall photovoltaic performance at different temperatures by keeping all other aspects identical.

2. Materials and methods

A water-bath dipping process carried out the temperature-dependent dye sensitization process. The fabricated ZnO photoanode was used for sensitization at various temperatures. As ZnO's optimized sensitization time is much shorter (4h) than TiO_2 (24h), therefore ZnO was chosen for this study. A more extended period of dye sensitization at a higher temperature may cause evaporation of the dye solution resulting in more dye degradation/agglomeration.

2.1. Synthesis of ZnO nanoparticles

Quasi-spherical ZnO nanoparticles (NPs) was synthesized by the sonochemical process using 250 mL 0.05(M) aqueous solution of Zinc nitrate hexahydrate [Zn $(NO_3)_2.6H_2O$, 99.9%] as zinc source where triethanolamine (TEA) was added dropwise, keeping the molar concentration of TEA to Zn^{2+} 1:1 with continuous stirring in magnetic stirrer at room temperature to make a homogeneous white slurry. Ammonium hydroxide (NH_4OH) was added dropwise as a precipitating agent to raise the solution's pH to 9±0.5 under ultrasonication. The as-prepared product was centrifuged at ~11,000 rpm washed with distilled water and ethanol to remove TEA and dried under the IR lamp. The as-prepared product was calcined at 450^oC for 4h to remove the residual template.

2.2. DSSC fabrication and temperature-dependent sensitization

The ZnO films fabricated by the screen printing (120T mesh/inch, Mascoprint, UK) method consist of a circular area of 0.2826 cm^2 on fluorine-doped tin oxide (FTO) (7 $\Omega.cm^{-2}$) glass substrate using a homemade paste with ethyl cellulose and α-terpinol (Sigma Aldrich). We used three layers of ZnO paste to fabricate the ZnO photoanode, followed by annealing under an ambient atmosphere following multiple heating steps (125^oC for 5min., 375^oC for 10min,

450^{o}C for 15 min, and then 500^{o}C for 20 min). For the dye adsorption, the ZnO films were soaked in the N719 dye (0.5 mM, Solaronix) in absolute ethanol (Merck, Germany) at a temperature range of 4h. The temperature-dependent dye sensitization process was followed a water-bath dipping process as schematically mention in Fig. 1. To maintain a constant and fixed temperature, a water batch component was introduced to keep the same. Inside the water bath chamber, the fabricated ZnO photoanode was allowed for the sensitization described in Fig. 1.

After the dye adsorption process, the films were thoroughly rinsed with absolute ethanol to remove the physically adsorbed excess dye molecules. Sandwich-type DSSCs were then assembled using the dye-adsorbed ZnO film and a platinized FTO substrate (by drop-casting) with a hot-melt film (~25 μm, Surlyn, Dyesol) between them. a Electrolyte preparation, 0.3M 1-methylbenzimidazole (NMB) was thoroughly mixed with 1:1 volume ratio containing acetonitrile and 3-methoxypropionitrile (MPN) solution. After that, 0.4M LiI, 0.4M tetrabutylammonium iodide (TBAI) and 0.04M I_2 was added to the above solution and constant stir overnight. All the chemicals used were brought from Sigma Aldrich and used without further purification. Finally, the prepared I_3^-/I^- liquid electrolyte was infiltrated into the cell and made a sandwiched DSSC device [20, 21].

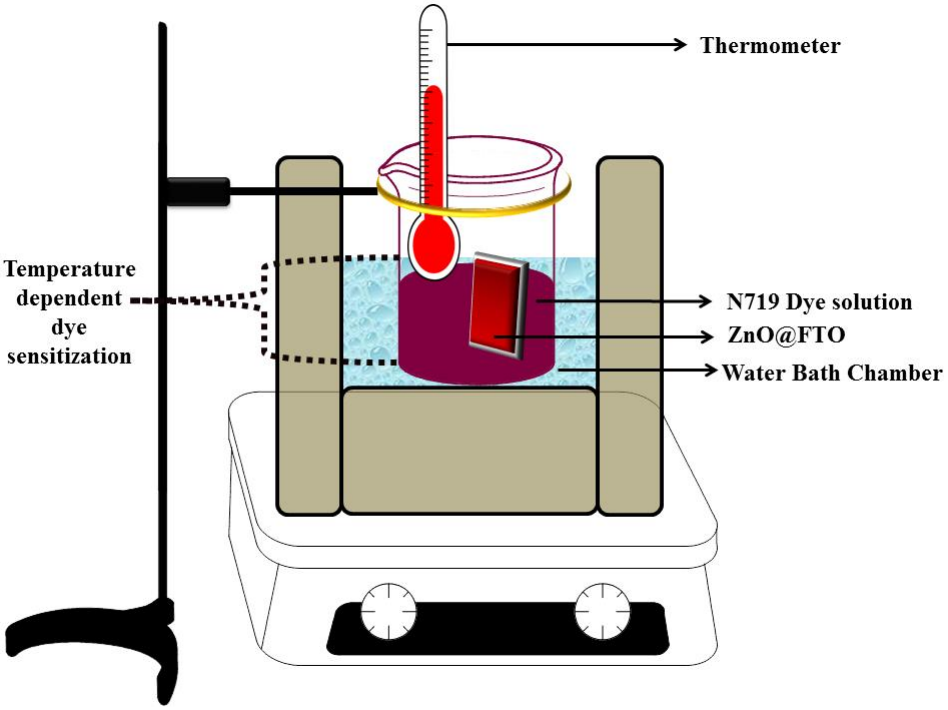

Fig. 1 Schematic representation of the dye-sensitization experiment for different temperature.

2.3. Material characterizations

The optical absorption spectra of the unadsorbed dye solutions and diffuse reflectance (DR) spectroscopy of the ZnO films were recorded on a UV-Vis-NIR spectrometer (Shimadzu UV-3600). The relative surface wettability of the ZnO films with N719 was accomplished by measuring the successive water contact angles (Cas) on a drop shape analyzer (Krüss DSA25) using Young's equation (sessile drop method). Zeta potential measurements were carried out on a Horiba Nanoparticle Analyzer-SZ100. Each drop's volume was fixed at 5 mL, and the dosing rate was 500 $mL.min^{-1}$. The instrument was equipped with a CCD camera for image capture. A PerkinElmer, Spectrum two Fourier transformed-infrared (FT-IR) spectrometer (with a resolution of 4 cm^{-1}) was used for the measurement using potassium bromide (FTIR grade ≥99%, Sigma-Aldrich). Morphology of the ZnO photoanodes was obtained on a field emission scanning electron microscope (FESEM) (LEO 430i, Carl Zeiss). The photocurrent density-voltage (*J-V*) characteristics were measured using an Agilent two-channel precision

source and measurement unit (model no. B2902A). The assembled devices' photovoltaic performances were measured under 1000 $W.m^{-2}$ light from a Wacom AAA continuous solar simulator (model WXS-210S-20, AM 1.5 G).

3. Results and Discussions

3.1. Optical analysis of temperature-dependent dye sensitization

The ZnO photoanodes were used for the temperature-dependent studies. A maximum of 6h sensitization period was fixed. It was observed that the dye loading capacity of ZnO varied for 5, 25 and 40^{o}C temperatures and beyond 40^{o}C, no significant improvement in dye loading behaviour for 60^{o}C temperature after 2h (Fig. 2a). Details of dye loading at different sensitization temperatures are given in a tabular form in Table 1. Further, dye CA measurements at each temperature were carried out to understand the dye's wettability at different sensitization temperatures, as shown in Fig. 2b. Ambade et al. (2009) have used CA measurement as an empirical diagnostic method to pre-evaluate the performance of ZnO based DSSC for the first time [22]. The formation of the inhomogeneous Zn^{2+}/dye complex on the surface changes the surface properties from comparatively hydrophobic to hydrophilic [23]. It was observed that with an increase in temperature from 5 to 60^{o}C, the dye CA did not follow any trend. The lowest CA observed at 40^{o}C was 8^{o} leading to a superhydrophobic nature. The highest dye CA recorded at 60^{o}C temperature was 42^{o}, exhibiting a more hydrophobic character. Following the dye contact angle measurements, zeta potential measurements of the N719 dye-sensitized ZnO powder dispersion was performed. Fig. 2b displays zeta possible measurements of the ethanolic dispersion of N719 dye adsorbed ZnO powder sensitized at different temperatures with negative values indicating the weak ZnO-N719 dye interaction. The maximum zeta potential observed was -35.2 mV by 40^{o}C sensitized film. The coating exhibited a low negative zeta potential of (-10 mV) at 60^{o}C. Therefore, 40^{o}C sensitized film

showed the highest negative zeta value and the most inferior dye CA. The recorded values of dye CA and zeta potential measurement for different sensitization temperature have been tabulated in Table 1. The CA variation with sensitization time indicates a good correlation with the dye molecules' stability in the presence of the photoanode. The CA measurements have been used to unequivocally establish the ZnO photoanode surface's stability with the N719 dye molecule.

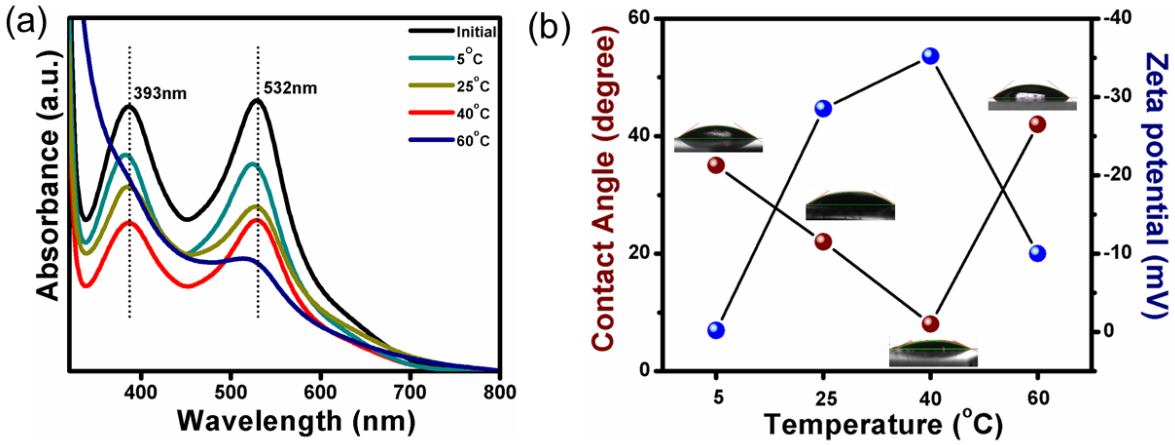

Fig. 2 (a) Plot of desorbed N719 dye's absorption spectra after 4h dipping during the sensitization of the fabricated ZnO photoanodes, and (b) plot of dye contact angle and zeta potential measurement.

Table 1. Various parameters for N719 dye sensitization on ZnO film at different temperatures.

Sensitizing Temperature (ºC)	**Amount of Dye Loading (µM.cm^{-2})**	**Zeta Potential (mV)**	**Water Contact Angle (º)**
5	12.36	-20	40
25	30.87	-28	24
40	40.82	-40	5
60	23.16	-12	47

The FTIR spectra of the N719 dye adsorbed on ZnO with different solution temperatures ranging from 5 to 60°C have been shown in Fig. 3. FTIR band of NCS was assigned at ~2094-2108 cm^{-1}. The FTIR transmittance at ~1455-1478 cm^{-1} can be ascribed to tetrabutylammonium

(TBA) counter-ions. It is also speculated that the TBA ions were separated from COO-TBAs in the dye solution to adsorb on the ZnO surface. The double FTIR bands of the COO group's symmetric vibration can also be seen ~1347-1372 cm^{-1}. The physisorbed bare N719 molecules, such as N719 powder on their own, exhibited the IR transmittance of COO at ~1346 cm^{-1}, while the chemically bonded N719 with bidentate or bridging linkage causes a shift to ~1375 cm^{-1}. The IR absorption peak of the COO- asymmetric vibration mode at wavenumbers from ~1607 to 1626 cm^{-1} can also be attributed to the two chemical states of physisorbed and chemisorbed N719 [15-18]. N719 dye adsorbs preferentially on the -OH sites on ZnO surfaces and makes bridges for electrons to the ZnO electrode with the bidentate or the bridging linkage. When the N719 dye solution temperature was increased from room temperature to 60°C, it enhanced the dye adsorption, as evident by the FTIR absorbance of NCS. Expanding the solution temperature enhances the chemisorbed state bidentate bonding, suggests power generation can be improved in DSSCs using a high-temperature dye solution. When the solution temperature was lowered from room temperature to 5^{o}C, the NCS peak remained with the same intensity as 25 and 40^{o}C. The physisorbed N719 offers shade to the chemisorbed N719 and suppresses the PCE. Thus, lowering the solution temperature is ineffective in improving the DSSC performance

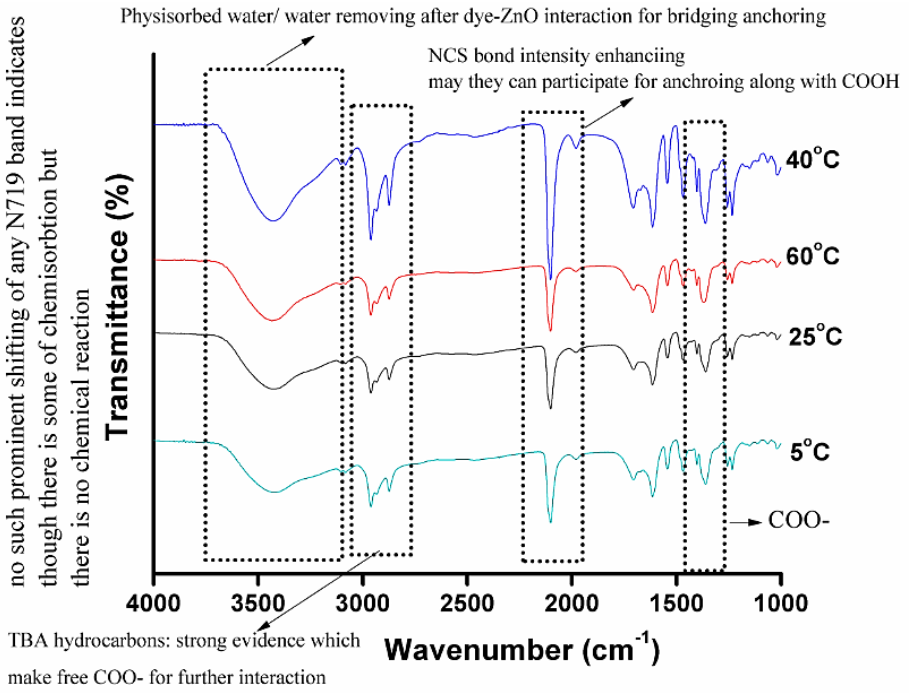

Fig. 3 FTIR spectra for N719 dye-sensitized ZnO films at 5, 25, 40 and 60ºC.

3.2. Microstructural and diffuse reflectance analysis of N719 dye-sensitized ZnO films

Fig.4a-d shows the typical scanning electron micrographs of N719 dye-sensitized ZnO electrodes on FTO at different solution temperatures. Fig. 4a corresponds to the FESEM surface microstructure of 5ºC temperature sensitized film followed by 25, 40, and 60ºC sensitized films (Fig. 4b-d), respectively. The unavoidable agglomeration increased as the solution temperature for sensitization was varied from 5 to 60ºC, respectively.

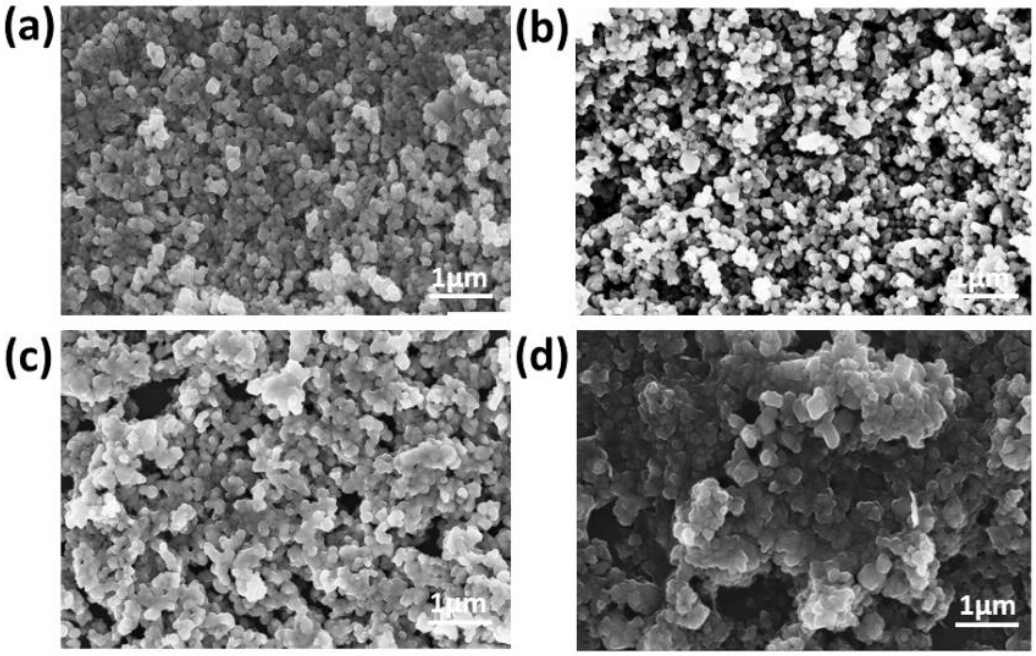

Fig. 4 SEM microstructural images of N719 dye sensitized ZnO films sensitized at (a) 5, (b) 25, (c) 40 and (d) 60^{o}C, respectively.

It is noticeable from the FESEM microstructural images that the degree of agglomeration increased on varying the sensitization temperature from 5 to 60^{o}C, as shown in Fig. 5a. To investigate the light-harvesting capacity of the different solution temperature of N719 dye-sensitized ZnO films prepared under different temperature, DR spectra were measured, as shown in Fig. 5b. The 40^{o}C sensitized ZnO film's absorption edge exhibited a significant blue shift. An abrupt decrease in the reflectance at around 380 nm corresponds to the inter-band absorption. The broad absorption band in the 520-560 nm range corresponds to the visible spectrum due to the N719 dyes' electronic excitation. The low reflectance for 40^{o}C sensitized film indicates the maximum adsorption of dye molecules on the ZnO surface, which is essential in improving the overall performance of DSSC [24, 25].

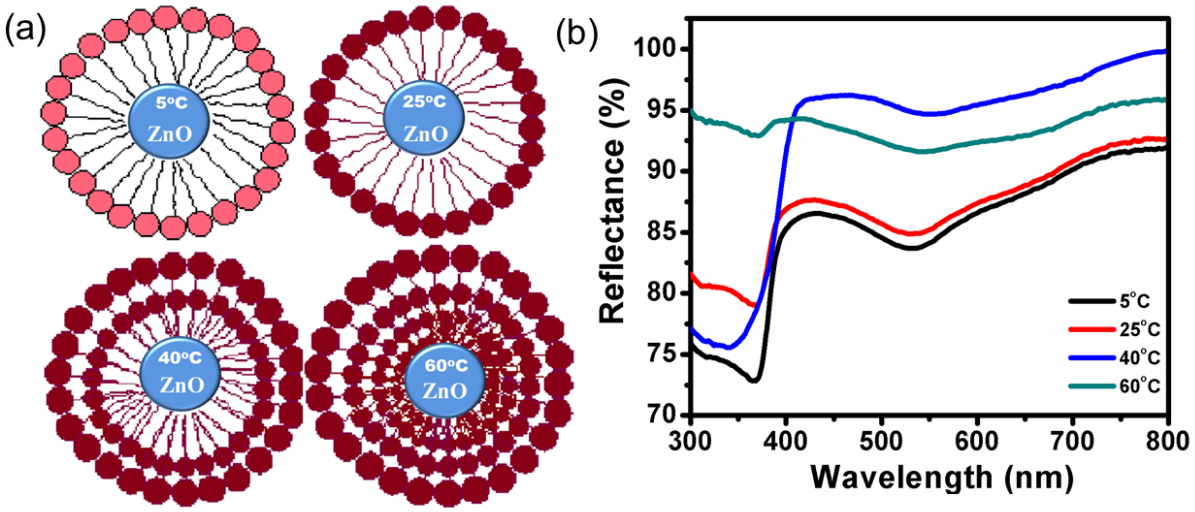

Fig.5 (a) Schematic representation of ZnO-N719 dye molecule surface agglomeration for different temperature, and (b) diffuse reflectance spectra of ZnO-photoanode, sensitized with N719 dye molecule at different temperature.

3.3. *I-V* Characteristics and Photovoltaic Performance

The *I-V* characteristics measured within the bias voltage of -40 to +40 V in Fig. 6a show a comparative status of the current generation at different temperature sensitized ZnO films at visible light with an ohmic response. The *I-V* characteristics sustain higher current generation for 60°C sensitized film, but 25 and 40°C sensitized films, on the other hand, shows almost similar performance on the current generation. The *J-V* characteristics of the DSSCs fabricated with N719 -sensitized ZnO films at 5, 25, 40 and 60°C temperature are exhibited in Fig. 6b. The detailed photovoltaic performances of the samples are summarized in Table 2. Interestingly, an ascending trend observed for J_{SC} and PCE, whether no such significant trend was observed for other parameters such as FF and V_{OC}.

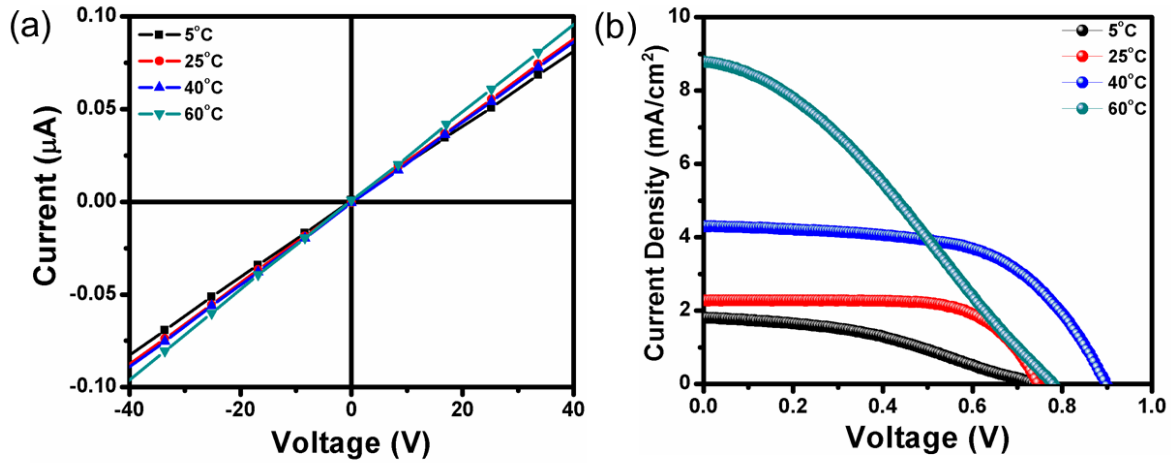

Fig. 6 (a) *I-V* characteristics of N719 dye-sensitized ZnO cells at different temperature and (b) *J-V* characteristics plot of N719 dye-sensitized at different sensitization temperature of the ZnO solar cells.

Table 2. Photovoltaic parameters of 4h N719 dye-sensitized ZnO solar cells at different sensitization temperature.

Sensitization Temperature (^{o}C)	**V_{OC} (V)**	**J_{SC} ±0.02 (mA.cm^{-2})**	**FF**	**PCE ±0.02 (%)**
5	0.74	1.81	0.38	0.51
25	0.75	2.72	0.69	1.16
40	0.87	4.29	0.61	2.26
60	0.78	8.79	0.32	2.19

The individual photovoltaic parameters have been shown as a bar diagram in Fig. 7a to understand those parameters' effect for different solution sensitized temperature. Fig. 7b indicates an ascending J_{SC} trend as with the sensitization temperature. The higher carrier concentration originated by ZnO attributed to the improved J_{SC} of 8.792 mA.cm^{-2} in the 60^{o}C sensitized film, which is more than double of 40^{o}C sensitized film, J_{SC} 4.293 mA.cm^{-2}. There is no significant change in the V_{OC} for all the cases except for the 40^{o}C sensitized film. It shows an exceptionally higher V_{OC} > 0.85V. In DSSCs, a variation of V_{OC} can be explained by (1) a shift of the potential of the ZnO conduction band edge and/or (2) a change of electron lifetime.

As electron lifetime decreases, recombination current increases, resulting in a decrease of V_{OC} and vice versa. The temperature dependence of V_{OC} exhibited a wide variation in V_{OC}, i.e., 0.72-0.85. The significant improvement in the FF attributes to a remarkable reduction in the recombination between the photoexcited carriers of photoanode and the $I^-/I_3^-$of the electrolyte at a temperature of 25°C, as shown in Fig. 7c. The deficient fill factor, higher short circuit current density owing to temperature increment, and favourable surface condition for dye adsorption related to the enhancement of surface basicity collectively account for the improved overall PCE. Besides, Fig. 7d indicates a sharp PCE enhancement once the sensitization temperature increases to 40°C. However, the PCE gets a steady decrement in PCE at a higher temperature, probably due to lower V_{OC} and FF.

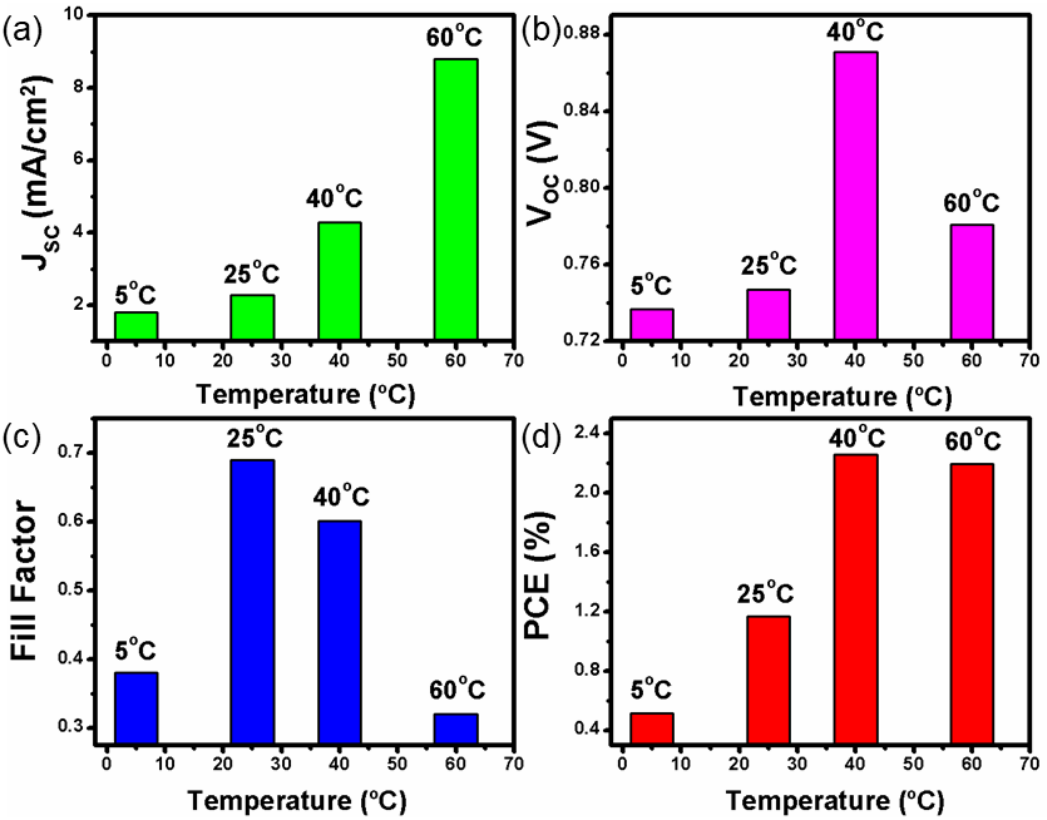

Fig. 7 Variation of photovoltaic parameters such as (a) short-circuit current density (J_{SC}), (ii) open-circuit voltage (V_{OC}), (Cc) fill factor (FF) and (d) power conversion efficiency (PCE) of ZnO-based DSSC concerning N719 dye sensitization temperature as 5, 25, 40 and 60°C, respectively.

4.4.6 Mode of N719 Dye Sensitization with ZnO

The structure of N719 dye has been shown in Fig. 8a. As shown in Fig.8b, the first type of binding, known as ester-type linkage, involves the interaction of one or two oxygen atoms of the -COOH group with the Zn atoms of the ZnO surface, resulting in unidentate or bidentate coordination mode. The second type of binding involves the interaction of both oxygen atoms of COOH groups with either one or two Zn atoms, resulting in bidentate chelating or bridging, as depicted in Fig. 8c and Fig. 8d, respectively. Carboxylate groups are expected to get attached to the ZnO surface via bidentate chelating or bridging coordination using two carboxylic acid groups per dye molecule. A third binding mechanism (Fig. 8e) was also proposed based on molecular dynamics simulations and electronic structure calculations. Accordingly, the N719 dye binding to the ZnO surface occurs through three carboxylic groups attached to two Zn atoms in bidentate form while the other two are bound via monodentate mode [26].

In contrast to these findings, a fourth binding mechanism (Fig. 8f) was also proposed. The N719 dye molecules interact with the TiO_2 surface through the NCS group and the bidentate bridging [27,28]. Based on detailed vibrational spectroscopic studies of N719 dye absorbed on the ZnO surface, they proposed that the binding of the dye to ZnO occurs through two neighbouring carboxylic acid/ carboxylate groups via a combination of bidentate bridging and H-bonding involving a donating group from the N719 dye and acceptor from the Zn-OH group (Fig. 8g). Though most studies suggest anchoring of N719 dye on the ZnO surface via two carboxylate groups, the role of various kinds of surface treatments of the ZnO surface has not been reported to date [29-31]. As the N719 dye sensitization temperature increases, it more efficiently binds with the ZnO, allowing free electron mobility and enhancing PCE. Simultaneously, the dye started to degrade or agglomerate at a higher temperature, which severely impactedthe severely impacted FF and VOC of the ZnO-based device. Therefore,

40^{o}C was considered an optimized sensitization condition at which reliable DSSC parameters were achieved.

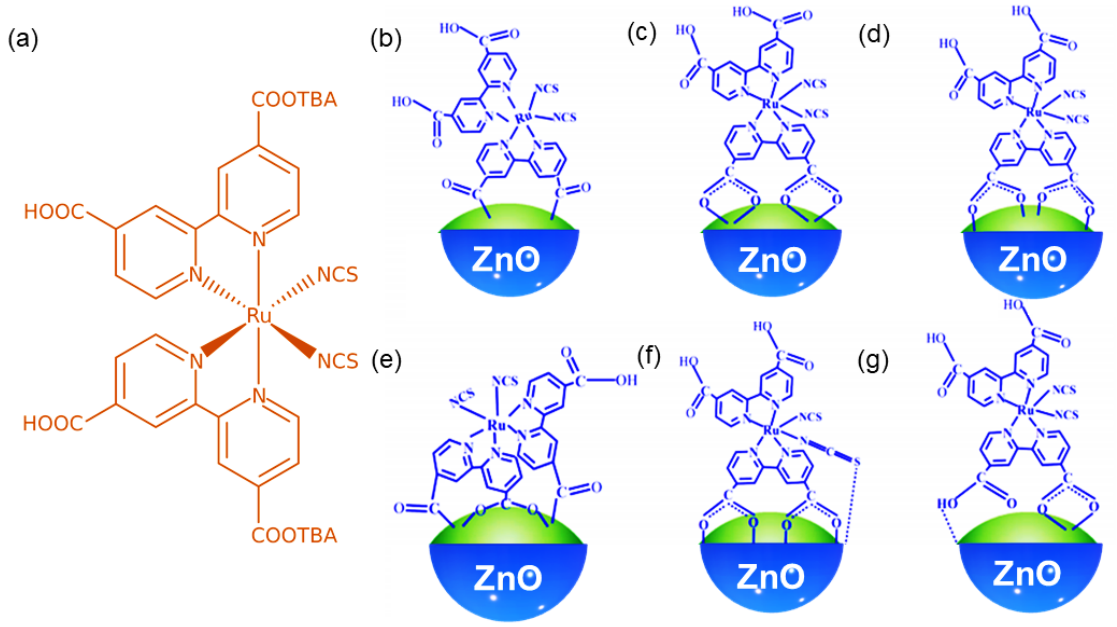

Fig. 8 (a) N719 dye structure and schematic presentations of binding of N719 dye on the ZnO surface: (b) ester linkage, (c) bidentate chelating, (d) bidentate bridging, (e) mixed bidentate and monodentate mode, (f) NCS group interacts with the ZnO surface, and (g) bidentate chelating and hydrogen bonding [26].

4. Conclusions

In summary, the insights of photo-physical surface characteristics for N719 dye sensitization and its performance in DSSC at different temperatures such as 5, 25, 40 and 60^{o}C for ZnO based photoanodes have been investigated in this part of the study. A significant influence of sensitization temperature over the solar cell's overall parameters and of PCE has been observed. The UV-Vis absorption spectral analysis, dye contact angle measurements, FTIR analysis and FESEM microstructural investigations were performed to understand the surface interaction behaviour of ZnO-N719 dye for different sensitization temperatures. Maximum PCE of 2.26% with an exceptionally high V_{OC} of 0.87V was recorded for 40^{o}C sensitized

device. 60^{o}C sensitization exhibited the highest current density of 8.792 mA.cm$^{-2,}$ and 25^{o}C sensitized device showed a maximum fill factor of 0.68. Therefore, the mode of surface interaction and further fruitful connection of N719-ZnO to promote better electron conduction is highlighted through these experiments. The development of adequate physicochemical understanding of photoanode sensitization further constitutes a priority for current and future research in this area. It is logically inferred that this valuable sensitization optimization strategy like temperature, dye deprotonation level, sensitizing solvent can be extended to other analogous structures and materials for DSSCs.

Acknowledgements

A.R. gratefully acknowledges CSIR-Central Glass and Ceramic Research Institute, Kolkata 700032, India, supporting material characterization. A.R. also acknowledges Newton-Bhabha PhD Placement Program 2016-2017. Authors also thankful to the College of Engineering, Mathematics and Physical Sciences, University of Exeter.

Conflict of Interest

The authors declare no conflict of interest.

References

[1] F. Sauvage, J.D. Decoppet, M. Zhang, S.M. Zakeeruddin, S. Comte, M. Nazeeruddin, P. Wang, M. Grätzel, J. Am. Chem. Soc. 133 (2011) 9304.

[2] U. Mehmooda, A. A. Ahmeda, F.A.A. Sulaimana, M.I. Malikb, F. Shehzadb, A.U. Khan, Renew. Sustain. Energy Reviews 79 (2017) 946.

[3] S. Ardo, G. Meyer, Chem. Soc. Rev. 38 (2009)115.

[4] D. B. Kuang, C. Klein, S. Ito, J. E. Moser, R. Humphry-Baker, N. Evans, F. Duriaux, C. Grätzel, S. M. Zakeeruddin, M. Gratzel, Adv. Mater. 19 (2007) 1133.

[5] S. A. Haque, E. Palomares, B. M. Cho, A. N. M. Green, N. Hirata, D. R. Klug, J. R. Durrant, J. Am. Chem. Soc. 127 (2005) 3456.

[6] K. Sharma, V. Sharma, S.S. Sharma, Nanoscale Res Lett 13 (2018) 381.

[7] S. Shalini, R. Balasundaraprabhu, T. Satish Kumar, N. Prabavathy, S. Senthilarasu S. Prasanna, Int. J. Energy Res. 40 (2016) 1303.

[8] M. Xu, W. Wang, Y. Zhong, X. Xu, J. Wang, W. Zhou, Z. Shao, J. Mater. Chem. A, 7 (2019) 17489.

[9] B. Tan, E. Toman, Y. Li, Y. Wu, J. Am. Chem. Soc., 2007, 129, 4162-4163.

[10] V. Thavasi, V. Renugopalakrishnan, R. Jose, S. Ramakrishna, Mater. Sci. Eng. R, 2009, 63, 81-99.

[11] J. K. Lee, M. Yang, Mater. Sci. Eng. B, 176 (2011)1142.

[12] F. Yan, L. Huang, J. Zheng, J. Huang, Z. Lin, F. Huang, M. Wei, Langmuir 26 (2010) 7153.

[13] R. Scholin, M. Quintana, E. M. J. Johansson, M. Hahlin, T. Marinado, A. Hagfeldt, H. Rensmo, H. J. Phys. Chem. C, 115 (2011)19274.

[14] H. Horiuchi, R. Katoh, K. Hara, M. Yanagida, S. Murata, H. Arakawa, M. Tachiya, J. Phys. Chem. B, 107 (2003) 2570.

[15] T. P. Chou, Q. Zhang, G. Cao, J. Phys. Chem. C, 111 (2007) 18804.

[16] K.E. Lee, M.A. Gomez, S. Elouatik, G.P. Demopoulos, Langmuir 26 (2010) 9574.

[17] F. Hirose, M. Shikaku, Y. Kimura, M.J. Niwano, Electrochem. Soc. 157 (2010) 1578.

[18] C. Yoshida, S. Nakajima, Y. Shoji, E. Itoh, K. Momiyama, K. Kanomata, F.J. Hirose, Electrochem. Soc. 159 (2012) 881.

[19] M. Berginc, U.O. Krašovec, M. Hočevar, M. Topič, Thin Solid Films 516 (2008) 7154.

[20] A. Roy, P.P. Das, P. Selvaraj, S. Sundaram, P.S. Devi, ACS Sustain. Chem. Eng. 6 (2018) 3299.

[21] A. Roy, P.P. Das, P. Selvaraj, S. Sundaram, P.S. Devi, J. Photochem. Photobiol. A, 380 (2019) 111824.

[22] S. B. Ambade, R. S. Mane, A. V. Ghule, M. G. Takwale, A. Aditya, B. W. Chod, S. H. Han, Scripta Materialia, 61 (2009) 12.

[23] P. P. Das, A. Roy, S. Das, P.S. Devi, Phys. Chem. Chem. Phys. 18 (2016) 1429.

[24] C.C. Ting, W.S. Chao, Measurement 43 (2010) 1623.

[25] F. Hirose, K. Kuribayashi, T. Suzuki, Y. Narita, K. Kimura, M. Niwano, Electrochem. Solid-State Lett. 11 (2008) 109.

[26] J. Singh, A. Gusain, V. Saxena, A.K. Chauhan, P. Veerender, S.P. Koiry, P. Jha, A. Jain, D.K. Aswal, S.K. Gupta, J. Phys. Chem. C 117 (2013) 21096.

[27] M.K. Nazeeruddin, R.H. Baker, P. Liska, M. Grätzel, J. Phys. Chem. B 107 (2003) 8981.

[28] C.P. León, L. Kador, B. Peng, M. Thelakkat, J. Phys. Chem. B 110 (2006) 8723.

[29] F.D. Angelis, S. Fantacci, A. Selloni, M.K. Nazeeruddin, M. Grätzel, J. Phys. Chem. C 114 (2010) 6054.

[30] E.M. J. Johansson, M. Hedlund, H. Siegbahn, H. Rensmo, J. Phys. Chem. B 109 (2005) 22256.

[31] P. Cheng, L. Feng, Y. Liu, D. Zheng, Y. Sang, W. Zhao, Y. Yang, S. Yang, D. Wei, G. Wang, Angew. Chem. Int. Ed. 59 (2020) 21414.

Table of Content

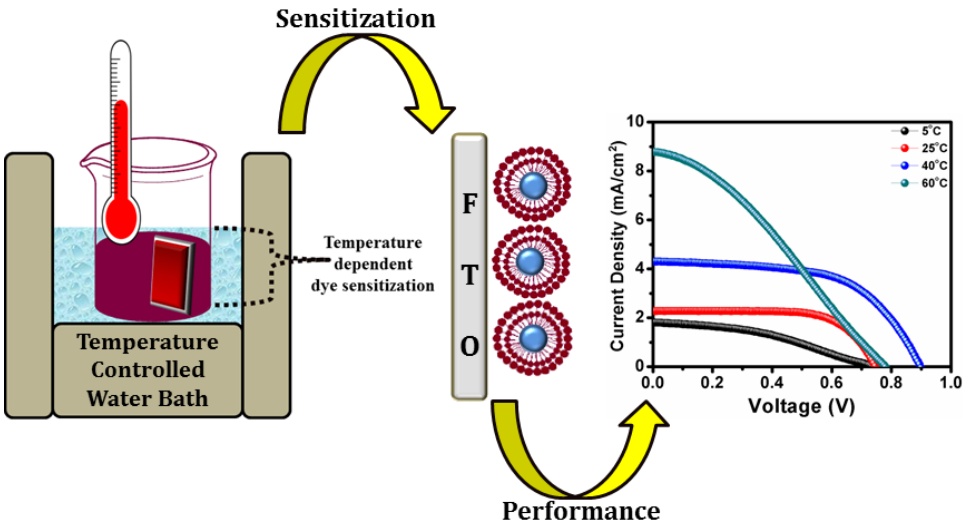

N719 dye sensitization-temperature depended on photovoltaic performance of ZnO photoanode.